Eur. Phys. J. C 18, 157–166 (2000)
Digital Object Identifier (DOI) 10.1007/s100520000502

THE EUROPEAN PHYSICAL JOURNAL C


# A theoretical prediction of the $B_s$ meson lifetime difference

D. Becirevic[1], D. Meloni[1], A. Retico[1], V. Giménez[2], V. Lubicz[3], G. Martinelli[4]

[1] Dip. di Fisica, Univ. di Roma "La Sapienza" and INFN, Sezione di Roma, P.le A. Moro 2, 00185 Roma, Italy
[2] Dep. de Física Teòrica and IFIC, Univ. de València, Dr. Moliner 50, 46100, Burjassot, València, Spain
[3] Dipartimento di Fisica, Università di Roma Tre and INFN, Sezione di Roma Tre, Via della Vasca Navale 84, 00146 Rome, Italy
[4] Centre de Physique Théorique de l'École Polytechnique, 91128 Palaiseau-Cedex, France

Received: 13 June 2000 / Published online: 13 November 2000 – © Springer-Verlag 2000

**Abstract.** We present the results of a quenched lattice calculation of the operator matrix elements relevant for predicting the $B_s$ width difference. Our main result is $(\Delta\Gamma_{B_s}/\Gamma_{B_s}) = (4.7 \pm 1.5 \pm 1.6) \times 10^{-2}$, obtained from the ratio of matrix elements $\mathcal{R}(m_b) = \langle \bar{B}^0_s|Q_S|B^0_s\rangle/\langle \bar{B}^0_s|Q_L|B^0_s\rangle = -0.93(3)^{+0.00}_{-0.01}$. $\mathcal{R}(m_b)$ was evaluated from the two relevant $B$ parameters $B_S^{\overline{\rm MS}}(m_b) = 0.86(2)^{+0.02}_{-0.03}$ and $B_{B_s}^{\overline{\rm MS}}(m_b) = 0.91(3)^{+0.00}_{-0.06}$, which we computed in our simulation.

## 1 Introduction

In the standard model, the width difference $(\Delta\Gamma_{B_s}/\Gamma_{B_s})$ of $B_s$ mesons is expected to be rather large and within reach of being measured in the near future. Recent experimental studies [1,2] already provide an interesting bound on this quantity. In particular, in [2] the limit $(\Delta\Gamma_{B_s}/\Gamma_{B_s}) < 0.31$ $(95\% C.L.)$ is quoted[1].

Theoretically, the prediction of $(\Delta\Gamma/\Gamma)_{B_s}$ relies on the use of the operator product expansion (OPE), where the large scale is provided by the heavy-quark mass [3]. All recent developments, including the calculation of the next-to-leading order (NLO) perturbative QCD corrections, have been discussed in great detail in [4–6]. The theoretical estimates are in the range $(\Delta\Gamma_{B_s}/\Gamma_{B_s}) = (5 \div 15)\%$ and crucially depend on the size of relevant hadronic matrix elements which must be computed non-perturbatively.

In this paper we present a new lattice calculation of the main contribution to $(\Delta\Gamma_{B_s}/\Gamma_{B_s})$. On the basis of our results, and using the expressions given below, we predict

$$\frac{\Delta\Gamma_{B_s}}{\Gamma_{B_s}} = (4.7 \pm 1.5 \pm 1.6) \times 10^{-2}, \tag{1}$$

where the last error is obtained by assuming an uncertainty of 30% on the $1/m_b$ corrections.

We now present the relevant formulae which have been used to get the prediction in (1). Up to and including $1/m_b$ corrections, the theoretical expression for $(\Delta\Gamma_{B_s}/\Gamma_{B_s})$ reads [4]

$$\frac{\Delta\Gamma_{B_s}}{\Gamma_{B_s}} = \frac{G_F^2 m_b^2}{12\pi m_{B_s}} |V_{cb}V_{cs}|^2 \tau_{B_s} (G(z)\langle Q_L(m_b)\rangle - G_S(z)\langle Q_S(m_b)\rangle + \delta_{1/m}\sqrt{1-4z}), \tag{2}$$

where $z = m_c^2/m_b^2$ and $G(z)$ and $G_S(z)$ are functions which have been computed in perturbation theory at the next-to-leading order (NLO) [6]. $\langle Q_{L,S}\rangle = \langle \bar{B}^0_s|Q_{L,S}|B^0_s\rangle$ are the hadronic matrix elements of the renormalized operators relevant at the lowest order in the heavy-quark expansion

$$\begin{aligned} Q_L &= \bar{b}^i\gamma^\mu(1-\gamma_5)s^i\bar{b}^j\gamma_\mu(1-\gamma_5)s^j \\ Q_S &= \bar{b}^i(1-\gamma_5)s^i\bar{b}^j(1-\gamma_5)s^j, \end{aligned} \tag{3}$$

where $i$ and $j$ are color indices. The last term in (2), $\delta_{1/m}(1-4z)^{1/2}$, represents the contribution of $1/m_b$ corrections.

In order to reduce the uncertainties of the theoretical predictions, it is convenient to consider the ratio of the width and mass differences of the $B^0_s$–$\bar{B}^0_s$ system

$$\frac{\Delta\Gamma_{B_s}}{\Delta m_{B_s}} = \frac{4\pi}{3}\frac{m_b^2}{m_W^2}\left|\frac{V_{cb}V_{cs}}{V_{ts}V_{tb}}\right|^2 \frac{1}{\eta_B(m_b)S_0(x_t)} \times \left(G(z) - G_S(z)\frac{\langle Q_S\rangle}{\langle Q_L\rangle} + \tilde{\delta}_{1/m}\right), \tag{4}$$

where $\eta_B(m_b)$ has been computed in perturbation theory to NLO [7] and $S_0(x_t)$ is the usual Inami–Lim function [8]. Note that, to make contact with [6], in the above formulae we used the $\overline{\rm MS}$ coefficient $\eta_B(m_b)$ instead of the standard $\eta_B$ of [7]. Consequently, the operators $Q_S$ and $Q_L$ are renormalized in the $\overline{\rm MS}$ (NDR) scheme. We see from (4) that $(\Delta\Gamma_{B_s}/\Delta m_{B_s})$ only depends on the ratio of matrix elements,

$$\mathcal{R}(m_b) = \frac{\langle Q_S\rangle}{\langle Q_L\rangle} = \frac{\langle \bar{B}^0_s|Q_S(m_b)|B^0_s\rangle}{\langle \bar{B}^0_s|Q_L(m_b)|B^0_s\rangle}, \tag{5}$$

[1] For this estimate, the average $B_s$ decay width was assumed to be the same as for $B_d$ mesons

which may, in principle, be directly determined on the lattice. The use of $\mathcal{R}$ is particularly convenient because dimensionless quantities are not affected by the uncertainty due to the calibration of the lattice spacing. One may also argue that many systematic errors, induced by discretization and quenching, cancel in the ratio of two similar amplitudes.

Finally, (4) allows one to express $(\Delta\Gamma_{B_s}/\Gamma_{B_s})$ in terms of

(i) perturbative quantities, encoded in the overall factor and in the functions $G(z)$ and $G_S(z)$,

(ii) a lattice measured quantity, $\mathcal{R}$ and

(iii) $\Delta m_{B_s}$ which will hopefully be precisely measured in the near future:

$$\frac{\Delta\Gamma_{B_s}}{\Gamma_{B_s}} = (\tau_{B_s}\Delta m_{B_s})^{(\mathrm{exp.})}\ K \times \Big(G(z) - G_S(z)\mathcal{R}(m_b) + \tilde{\delta}_{1/m}\Big), \qquad (6)$$

where

$$K = \frac{4\pi}{3}\frac{m_b^2}{m_W^2}\left|\frac{V_{cb}V_{cs}}{V_{ts}V_{tb}}\right|^2 \frac{1}{\eta_B(m_b)S_0(x_t)}, \qquad (7)$$

Pending the measurement of $\Delta m_{B_s}$, for which only a lower bound presently exists [9], one can use a modified version of (6), namely

$$\frac{\Delta\Gamma_{B_s}}{\Gamma_{B_s}} = \left(\tau_{B_s}\Delta m_{B_d}\frac{m_{B_s}}{m_{B_d}}\right)^{(\mathrm{exp.})}\left|\frac{V_{ts}}{V_{td}}\right|^2 \times K\cdot(G(z) - G_S(z)\mathcal{R}(m_b) + \tilde{\delta}_{1/m})\xi^2, \qquad (8)$$

where

$$\xi = \frac{f_{B_s}\sqrt{\hat{B}_{B_s}}}{f_{B_d}\sqrt{\hat{B}_{B_d}}}. \qquad (9)$$

In this way, besides the quantities discussed above, we only use the experimental $B_d$ meson mass difference, which is known with a tiny error [2]

$$(\Delta m_{B_d})^{(\mathrm{exp.})} = 0.484(15)\mathrm{ps}^{-1}, \qquad (10)$$

and another ratio of hadronic matrix elements, namely $\xi$, which is rather accurately determined in lattice simulations [10,11].

For the following discussion, it is useful to write (8) as (note the $\mathcal{R}(m_b)$ is negative)

$$\frac{\Delta\Gamma_{B_s}}{\Gamma_{B_s}} = \big[(0.5\pm0.1) - (13.8\pm2.8)\mathcal{R}(m_b) + (15.7\pm2.8)\tilde{\delta}_{1/m}\big]\times10^{-2}, \qquad (11)$$

where the three contributions correspond to $G(z)$, $-G_S(z)\mathcal{R}(m_b)$ and $\tilde{\delta}_{1/m}$ in (8), respectively.

The advantage of using (4), (6) and (8) consists also in the fact that, in order to predict $(\Delta\Gamma_{B_s}/\Gamma_{B_s})$, we do not need $f_{B_s}$, which enters (2) when we express the matrix elements in terms of $B$ parameters. There is still a considerable uncertainty, indeed, on $f_{B_s}$, which has been evaluated both in the quenched ($f_{B_s} = 195\pm20\,\mathrm{MeV}$) and unquenched ($f_{B_s} = 245\pm30\,\mathrm{MeV}$) case, with a sizable shift between the two central values [10]. Since the "unquenched" results are still in their infancy, however, we think that the large quenching effect should not be taken too serious yet.

In the numerical evaluation of the width difference, we have used the values and errors of the parameters given in Table 1. For the perturbative quantities $G(z)$ and $G_S(z)$, the main uncertainty comes from the dependence on the renormalization scale, which was varied between $m_b/2$ and $2m_b$ in [6] (with $m_b = 4.8\,\mathrm{GeV}$). For this reason, we found it useless to recompute these coefficients with $m_b = 4.6\,\mathrm{GeV}$ (which is very close to the mass used in [6] ). Instead, we took as central value the average $G_S(z) = (G_S^{\mu_1=m_b/2}(z) + G_S^{\mu_1=2m_b}(z))/2$ (see Table 1 of that paper), and as error $(G_S^{\mu_1=m_b/2}(z) - G_S^{\mu_1=2m_b}(z))/2$. The same was done in the case of $G(z)$.

For the hadronic quantities, we have used the following values:

$$\mathcal{R}(m_b) = -0.93(3)^{+0.00}_{-0.01}, \quad \xi = 1.16(7); \qquad (12)$$

$\mathcal{R}(m_b)$ is the main result of this lattice study, while the result for $\xi$ has already been reported in our previous paper [11]. Following [4], for the $1/m_b$ corrections we get

$$\delta_{1/m} = -2.0\,\mathrm{GeV}^4, \qquad (13)$$

using $f_{B_s} = 204\,\mathrm{MeV}$ from [11]. This value of $\delta_{1/m}$ corresponds to $\tilde{\delta}_{1/m} = -0.55$ (obtained with $B_{B_s}^{\overline{\mathrm{MS}}}(m_b) = 0.91$)[2]. Since in the estimate of $\tilde{\delta}_{1/m}$, the operator matrix elements were computed in the vacuum saturation approximation (VSA), and the radiative corrections were not included, we allow it to vary by 30%, i.e. $\tilde{\delta}_{1/m} = -0.55\pm0.17$. In the numerical evaluation of the factor $K$, we have used the pole mass $m_b = 4.6\,\mathrm{GeV}$ derived from the $\overline{\mathrm{MS}}$ mass in Table 1 at the NLO. Using these numbers, from (8) we obtain the result in (1), where the last error comes from the uncertainty on $\tilde{\delta}_{1/m}$.

We have an important remark to make. Equation (11) shows explicitly the cancellation occurring between the main contribution, proportional to $\mathcal{R}(m_b)$, and the $1/m_b$ corrections, proportional to $\tilde{\delta}_{1/m}$. Without the latter, we would have found a much larger value, $(\Delta\Gamma_{B_s}/\Gamma_{B_s}) \simeq 14\times10^{-2}$. $(\Delta\Gamma_{B_s}/\Gamma_{B_s})$ would remain in the 10% range even with a sizable, but smaller, value for the $1/m_b$ term, $\tilde{\delta}_{1/m} = -0.30$ for example. This demonstrates that, in spite of the progress made in the evaluation of the relevant matrix elements ($\langle Q_S\rangle$ and $\langle Q_L\rangle$), a precise determination

[2] In [11], we gave $B_{B_s}^{\overline{\mathrm{MS}}}(m_b) = 0.92(3)^{+0.00}_{-0.06}$. The tiny difference is due to the fact that there, in the perturbative evolution, we used a number of flavours $n_f = 4$ instead of $n_f = 0$ as in the present paper

**Table 1.** Average and errors of the main parameters. When the error is negligible it has been omitted. The heavy-quark masses ($m_t$, $m_b$ and $m_c$) are the $\overline{\rm MS}$ masses renormalized at their own values, e.g. $m_t = m_t^{\overline{\rm MS}}(m_t^{\overline{\rm MS}})$. $m_s = m_s^{\overline{\rm MS}}(\mu = 2\,{\rm GeV})$ is the strange quark mass renormalized in $\overline{\rm MS}$ at the scale $\mu = 2\,{\rm GeV}$. Its central value and error are not important in the numerical evaluation of $\Delta\Gamma_{B_s}$

| Parameter | Value and error |
|---|---|
| $m_W$ | $80.41\,{\rm GeV}$ |
| $m_{B_d}$ | $5.279\,{\rm GeV}$ |
| $m_{B_s}$ | $5.369\,{\rm GeV}$ |
| $\tau_{B_s}$ | $1.460 \pm 0.056\,ps$ |
| $\lvert V_{cb}\rvert$ | $0.0395 \pm 0.0017$ |
| $\lvert V_{ts}\rvert$ | $0.0386 \pm 0.0013$ |
| $\lvert V_{cs}\rvert$ | $0.9759 \pm 0.0005$ |
| $\lvert V_{td}\rvert$ | $0.0080 \pm 0.0005$ |
| $\alpha_{\rm s}(M_Z)$ | $0.118 \pm 0.003$ |
| $\Delta m_{B_d}$ | $0.484 \pm 0.015\,{\rm ps}^{-1}$ |
| $m_t$ | $165 \pm 5\,{\rm GeV}$ |
| $m_b$ | $4.23 \pm 0.07\,{\rm GeV}$ |
| $m_c/m_b$ | $0.29 \pm 0.02$ |
| $m_s$ | $110 \pm 20\,{\rm MeV}$ |
| $\eta_B(m_b)$ | $0.85 \pm 0.02$ |
| $G(z)$ | $0.030 \pm 0.007$ |
| $G_S(z)$ | $0.88 \pm 0.14$ |

of the width difference requires a good control of the subleading terms in the $1/m_b$ expansion, which is missing to date.

One can also use (6), and combine it with [9]

$$(\Delta m_{B_s})^{(\rm exp.)} > 14.6\,{\rm ps}^{-1}, \tag{14}$$

to obtain a lower bound on $(\Delta\Gamma_{B_s}/\Gamma_{B_s})$. Given the large uncertainties, this bound is at present rather weak. At the $1\sigma$ level we get

$$\frac{\Delta\Gamma_{B_s}}{\Gamma_{B_s}} > 2.5 \times 10^{-2}\ (68\%{\rm C.L.}). \tag{15}$$

Following [2], from (6) and the limit $(\Delta\Gamma_{B_s}/\Gamma_{B_s}) < 0.31$, we could also obtain an upper limit on $\Delta m_{B_s}$. In our case this is not very interesting, however, since we find a very large upper bound of $\mathcal{O}(200)\,{\rm ps}^{-1}$.

Our prediction in (1) is in good agreement with [6]. It is instead about a factor of two smaller than the result of [17]. A detailed comparison of the two lattice calculations can be found in Sect. 4.

We stress that the theoretical formulae should be evaluated with hadronic parameters computed in a coherent way, within the same lattice calculation, and not from different calculations (the "Arlequin" procedure according to [12]), since their values and errors are correlated. All our lattice results were obtained using a non-perturbatively improved action [13], and with operators renormalized on the lattice with the non-perturbative method of [14], as implemented in [15,16]. Our new result is $\mathcal{R}(m_b)$. For completeness, we also present some relevant $B$ parameters which enter the calculation of the mixing and width difference

$$B_S^{\overline{\rm MS}}(m_b) = 0.86(2)^{+0.02}_{-0.03}, \quad B_{B_s}^{\overline{\rm MS}}(m_b) = 0.91(3)^{+0.00}_{-0.06}. \tag{16}$$

The remainder of this paper is as follows: in Sect. 2 we discuss the renormalization of the relevant operators and the calculation of their matrix elements; the extrapolation to the physical points and the evaluation of the statistical and systematic errors are presented in Sect. 3; Sect. 4 contains a comparison of our results with other calculations of the same quantities as well as our conclusions.

## 2 Calculation of the matrix elements

In this section, we discuss the construction of the renormalized operators which enter the prediction of $\Delta\Gamma_{B_s}$ and describe the extraction of their matrix elements in our simulation.

Besides the operators in (3), we also need

$$\begin{aligned} \tilde{Q}_S &= \bar{b}^i(1-\gamma_5)s^j\bar{b}^j(1-\gamma_5)s^i, \\ Q_P &= \bar{b}^i(1-\gamma_5)s^i\bar{b}^j(1+\gamma_5)s^j, \\ \tilde{Q}_P &= \bar{b}^i(1-\gamma_5)s^j\bar{b}^j(1+\gamma_5)s^i. \end{aligned} \tag{17}$$

The five operators in (3) and (17) form a complete basis necessary for the lattice subtractions which will be discussed later on. In [18], a new method, that allows the calculation of $\Delta F = 2$ amplitudes without subtractions, has been proposed and feasibility studies are underway. If successful, it obviously will be applied also to the calculation of $\Delta\Gamma_{B_s}$.

The matrix elements which contribute to $\Delta\Gamma_{B_s}$ are traditionally computed in terms of their value in the vacuum saturation approximation (VSA), by introducing the so-called $B$ parameters. The latter encode the mismatch between full QCD and VSA values. There is a certain freedom in defining the $B$ parameters (see for example the discussion in [19]). For $Q_S$ and $\tilde{Q}_S$, two equivalent definitions will be used in the following:

$$\begin{aligned} &\langle \bar{B}_q^0|Q_L(\mu)|B_q^0\rangle = \frac{8}{3}m_{B_s}^2 f_{B_s}^2 B_{B_s}(\mu), \\ &\langle \bar{B}_q^0|Q_S(\mu)|B_q^0\rangle = -\frac{5}{3}\left(\frac{m_{B_s}}{m_b(\mu)+m_s(\mu)}\right)^2 m_{B_s}^2 f_{B_s}^2 \\ &\times B_S(\mu) \equiv -\frac{5}{3}m_{B_s}^2 f_{B_s}^2 B'_S(\mu), \\ &\langle \bar{B}_q^0|\tilde{Q}_S(\mu)|B_q\rangle = \frac{1}{3}\left(\frac{m_{B_s}}{m_b(\mu)+m_s(\mu)}\right)^2 m_{B_s}^2 f_{B_s}^2 \\ &\times \tilde{B}_S(\mu) \equiv \frac{1}{3}m_{B_s}^2 f_{B_s}^2 \tilde{B}'_S(\mu). \end{aligned} \tag{18}$$

The first definition is the traditional one that requires, for the physical matrix elements, the knowledge of the

**Table 2.** Numerical results for the $\Delta(g_0^2)$s and the matrix $Z(g_0^2,\mu)$. They have been evaluated non-perturbatively in the Landau RI-MOM scheme, at $\beta = 6/g_0^2 = 6.2$, at the three different scales $\mu$ given in the table

| Scale $\mu$ | $\Delta_L$ | $\Delta_P$ | $\Delta_{\tilde{P}}$ | $\widetilde{\Delta}_L$ | $\widetilde{\Delta}_P$ | $\widetilde{\Delta}_{\tilde{P}}$ |
|---|---|---|---|---|---|---|
| 1.9 GeV | 0.005(1) | 0.219(8) | -0.016(8) | -0.002(0) | -0.094(3) | 0.007(3) |
| 2.7 GeV | 0.003(0) | 0.175(5) | -0.014(2) | -0.001(0) | -0.075(2) | 0.005(1) |
| 3.8 GeV | 0.002(1) | 0.189(3) | -0.012(2) | -0.001(0) | -0.081(1) | 0.003(1) |

| Scale $\mu$ | $Z_{22}(\mu)$ | $Z_{23}(\mu)$ | $Z_{32}(\mu)$ | $Z_{33}(\mu)$ |
|---|---|---|---|---|
| 1.9 GeV | 0.237(13) | -0.122(16) | 0.313(1) | 1.018(5) |
| 2.7 GeV | 0.282(12) | -0.128(16) | 0.229(0) | 0.883(3) |
| 3.8 GeV | 0.332(12) | -0.184(16) | 0.203(1) | 0.902(0) |

quark masses; the second one may present some advantage, because the matrix elements are derived using physical quantities only ($m_{B_s}$ and $f_{B_s}$). The label ($\mu$) denotes that operators and quark masses are renormalized, in a given renormalization scheme ($\overline{\rm MS}$ in our case) at the scale $\mu$. Since the matrix element of the first operator, essential for $\bar{B}_s^0$–$B_s^0$ mixing, was studied in detail in our previous paper [11], here we only consider the two other relevant operators, namely $Q_S$ and $\tilde{Q}_S$.

### 2.1 Matrix elements from correlation functions

Before presenting our results, let us recall the main steps necessary to extract the matrix elements in numerical simulations. As usual, one starts from the (Euclidean) three-point correlation functions:

$$\mathcal{C}_i^{(3)}(t_{P_1},t_{P_2}) = \sum_{\mathbf{x},\mathbf{y}} \langle 0|P_5(\mathbf{x},-t_{P_2})Q_i(0)P_5(\mathbf{y},t_{P_1})|0\rangle, \quad (19)$$

where $Q_i$ denotes any of the operators enumerated in (3) and (17). When the $Q_i$ and the sources $P_5$ (which we choose to be $P_5 = \mathrm{i}\bar{s}\gamma_5 b$) are sufficiently separated in time, the lightest pseudoscalar-meson contribution dominates the correlation functions and the matrix elements can be extracted

$$\mathcal{C}_i^{(3)}(t_{P_1},t_{P_2}) \overset{t_{P_1},t_{P_2}\gg 0}{\longrightarrow} \frac{\sqrt{\mathcal{Z}_P}}{2M_P} \times \mathrm{e}^{-M_P t_{P_1}} \langle \bar{P}|Q_i(a)|P\rangle \frac{\sqrt{\mathcal{Z}_P}}{2M_P} \mathrm{e}^{-M_P t_{P_2}}, \quad (20)$$

where $\mathcal{Z}_P^{1/2} = |\langle 0|P_5|P\rangle|$. We take both mesons at rest and label the bare operators on the lattice as $Q_i(a)$, to distinguish them from their continuum counterparts. The matching to the continuum renormalized operators is what we discuss next.

### 2.2 Operator matching and renormalization

In this subsection, we describe the procedure used to get the renormalized operator $Q_S(\mu)$, relevant in the calculation of $\Delta\Gamma_{B_s}$, from the lattice bare operators. This is achieved through a two steps procedure:

(i) We define the subtracted operators $Q'_S$ and $\tilde{Q}'_S$, obeying to the continuum Ward identities (up to corrections of $\mathcal{O}(a)$), as

$$Q'_S = Q_S(a) + \sum_{i=L,P,\tilde{P}} \Delta_i(g_0^2)Q_i(a)\ ,$$
$$\tilde{Q}'_S = \tilde{Q}_S(a) + \sum_{i=L,P,\tilde{P}} \widetilde{\Delta}_i(g_0^2)Q_i(a)\ . \quad (21)$$

The constants $\Delta_i(g_0^2)$, which we calculate using the non-perturbative method discussed in [15,16], are listed in Table 2. Note that the mixing (21) is a lattice artifact (as a consequence of the explicit chiral symmetry breaking in the Wilson action) and the subtraction ensures that the resulting operators, $Q'_S$ and $\tilde{Q}'_S$, have the same chiral properties as in the continuum.

In principle, the mixing coefficients $\Delta_i(g_0^2)$ are functions of the bare coupling constant $g_0^2$ only. Therefore, at fixed lattice spacing, they should be independent of the scale at which the operators are renormalized. In practice, due to some systematic effects, they may depend on the renormalization scale (which corresponds to the virtuality of the external quark legs). This induces an uncertainty in the determination of the physical matrix elements which will be accounted for in the estimate of the systematic error.

(ii) $CPS$ symmetry allows the mixing of $Q_S$ and $\tilde{Q}_S$ under renormalization. This is why we must consider both of them, although our main target is the matrix element of the renormalized $Q_S(\mu)$. In the second step, the operators are renormalized as

$$\begin{pmatrix} Q_S(\mu) \\ \tilde{Q}_S(\mu) \end{pmatrix} = \begin{pmatrix} Z_{22}(\mu)\ Z_{23}(\mu) \\ Z_{32}(\mu)\ Z_{33}(\mu) \end{pmatrix} \begin{pmatrix} Q'_S \\ \tilde{Q}'_S \end{pmatrix}, \quad (22)$$

where the structure of the mixing ($Z_{23} \neq Z_{32} \neq 0$) is the same as in the continuum. We compute the renormalization matrix non-perturbatively by using the method of [16], in the Landau RI-MOM renormalization scheme. The results for three values of the renormalization scale, $\mu = \{1.9\,\mathrm{GeV}, 2.7\,\mathrm{GeV}, 3.8\,\mathrm{GeV}\}$, are given in Table 2.

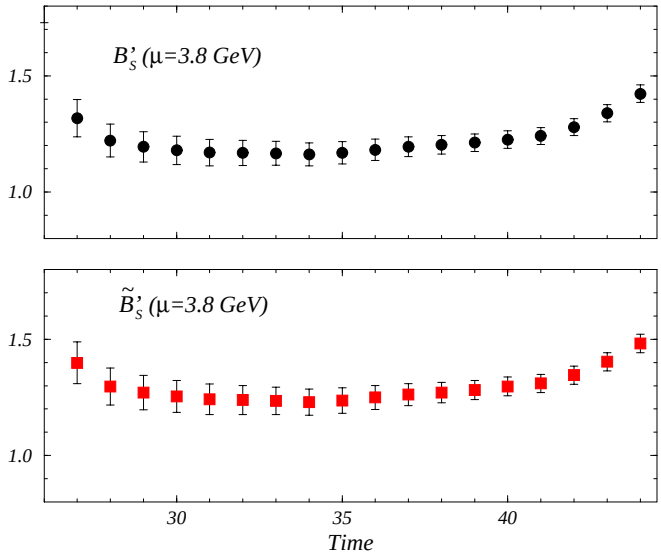


**Fig. 1.** The ratios defined in (23) are shown as a function of Time $= -t_{P_2}$ at fixed $t_{P_1} = 16$. All quantities are in lattice units. The figure refers to $\kappa_q = 0.1349$ and $\kappa_Q = 0.1220$

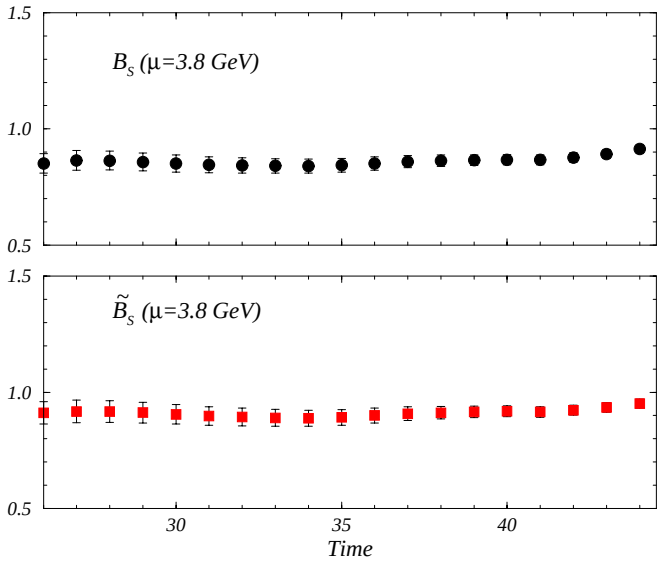


**Fig. 2.** As in Fig. 1 for the standard $B_S$ and $\tilde{B}_S$, as specified in (24)

### 2.3 Extraction of the $B$ parameters

Equipped with suitably renormalized operators in the RI-MOM scheme, we proceed by removing the external meson propagators and sources from the correlation functions. This can be done in two ways. From the ratios

$$\frac{\mathcal{C}_S^{(3)}(t_{P_1},t_{P_2};\mu)}{-\frac{5}{3}Z_A^2\mathcal{C}_{AP}^{(2)}(t_{P_2})\mathcal{C}_{AP}^{(2)}(t_{P_1})} \to \frac{\langle\bar{P}|Q_S(\mu)|P\rangle}{-\frac{5}{3}|\langle 0|\hat{A}_0|P\rangle|^2} \equiv B'_S(\mu),$$
$$\frac{\mathcal{C}_{\tilde{S}}^{(3)}(t_{P_1},t_{P_2};\mu)}{\frac{1}{3}Z_A^2\mathcal{C}_{AP}^{(2)}(t_{P_2})\mathcal{C}_{AP}^{(2)}(t_{P_1})} \to \frac{\langle\bar{P}|\tilde{Q}_S(\mu)|P\rangle}{\frac{1}{3}|\langle 0|\hat{A}_0|P\rangle|^2} \equiv \tilde{B}'_S(\mu), \tag{23}$$

we extract the $B'$ parameters (Method-I). The quality of the resulting plateaus is illustrated in Fig. 1. Since the lattice renormalization constant of the axial current ($\hat{A}_0 = Z_A\bar{s}\gamma_0\gamma_5 b$) is $\mu$ independent, the anomalous dimension of the parameter $B'_S(\mu)$ is exactly the same as for $\langle Q_S(\mu)\rangle$.

On the other hand, if we combine the correlation functions in the ratios

$$\frac{\mathcal{C}_S^{(3)}(t_{P_1},t_{P_2};\mu)}{-\frac{5}{3}Z_P^2(\mu)\mathcal{C}_{PP}^{(2)}(t_{P_2};\mu)\mathcal{C}_{PP}^{(2)}(t_{P_1};\mu)} \to \frac{\langle\bar{P}|Q_S(\mu)|P\rangle}{-\frac{5}{3}|\langle 0|\hat{P}_5(\mu)|P\rangle|^2}$$
$$\equiv B_S(\mu),$$
$$\frac{\mathcal{C}_{\tilde{S}}^{(3)}(t_{P_1},t_{P_2};\mu)}{\frac{1}{3}Z_P^2(\mu)\mathcal{C}_{PP}^{(2)}(t_{P_2};\mu)\mathcal{C}_{PP}^{(2)}(t_{P_1};\mu)} \to \frac{\langle\bar{P}|\tilde{Q}_S(\mu)|P\rangle}{\frac{1}{3}|\langle 0|\hat{P}_5(\mu)|P\rangle|^2}$$
$$\equiv \tilde{B}_S(\mu). \tag{24}$$

we get the standard $B$ parameters (Method-II). The plateaus are shown in Fig. 2.

In the above ratios, we have used the renormalized pseudoscalar density, $\hat{P}_5(\mu) = \mathrm{i}Z_P(\mu)\bar{s}\gamma_5 b$. The value of $Z_P(\mu)$ is also obtained non-perturbatively in the way described in [14]. Numerically (and in the chiral limit), we have $Z_P(\mu) = \{0.43(2), 0.45(2), 0.50(2)\}$ in increasing order of $\mu$.

The second method has the advantage that the (rather large) $\mu$ dependence of the operator $\langle Q_S(\mu)\rangle$ is almost cancelled by the anomalous dimension of the squared renormalized pseudoscalar density. On the other hand, the first method seems more convenient because physical amplitudes can be obtained without introducing the quark masses, which are a further source of theoretical uncertainty. We found, however, that $B'_S$ has a very strong dependence on the heavy-quark mass, which prevents a reliable extrapolation to $m_{B_s}$. Before discussing the subtleties related to the extrapolation, we present our results for the heavy-light meson masses directly accessible in our simulation.

### 2.4 $B$ parameters in the landau RI-MOM scheme

In this subsection we present the results for both sets of $B$ parameters. As in our previous paper [11], our study is based on a sample of 200 independent quenched gauge field configurations, generated at the coupling constant $\beta = 6.2$, on the volume $24^3 \times 48$. We use three values of the hopping parameter corresponding to the light-quark mass ($\kappa_q = 0.1344,\ 0.1349,\ 0.1352$), and three values corresponding to the heavy quarks ($\kappa_Q = 0.125, 0.122, 0.119$). The first source is kept fixed at $t_{P_1} = 16$, while the second one moves along the temporal axis. The 4-fermion operator under study is inserted at the origin ($t = 0$). After examining the plateaus of the different ratios in (23) and (24), for every combination of the hopping parameters, we choose to make the fit for the time intervals $t_{B_S} \in [31, 34]$ and $t_{\tilde{B}_S} \in [32, 35]$. We present results for each value of $\kappa_Q$, with the light quark interpolated to the $s$-quark or extrap-

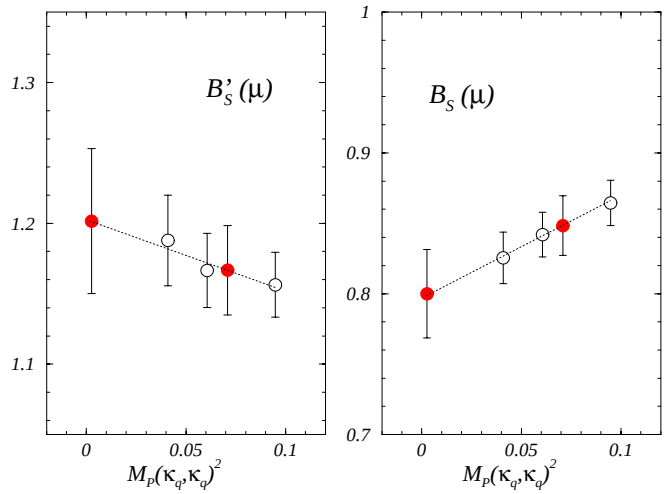


**Fig. 3.** Fit in the light-quark mass of $B_S(\mu)$ and $B'_S(\mu)$ (at $\mu = 3.8\,\mathrm{GeV}$) according to (25). Empty symbols denote data obtained from our simulation, whereas filled symbols denote quantities obtained after interpolation (extrapolation) to the strange (up-down) light-quark mass. The heavy-quark mass corresponds to $\kappa_{Q_2} = 0.1220$

olated to the $d$-quark. For a generic $B$-parameter, this is obtained by fitting our data to the following expression:

$$B(m_Q, m_q) = \alpha_0^Q + \alpha_1^Q M_P^2(m_q, m_q). \tag{25}$$

This is illustrated in Fig. 3, while a detailed list of results is presented in Tables 3 and 4.

At this point we have obtained the matrix elements parameterized in two ways ($B'_S(\mu)$–$\tilde{B}'_S(\mu)$ and $B_S(\mu)$–$\tilde{B}_S(\mu)$, respectively) in the RI-MOM scheme, at three values of the heavy-quark masses (around the charm quark mass). The matrix elements that we need refer, instead, to the $\overline{\mathrm{MS}}$ scheme and to the heavy mesons $B_s$. Thus, to get the physical results, we have to discuss the scheme dependence, and the extrapolation in the heavy-meson mass.

## 3 The physical mixing amplitudes

In this section we discuss the scaling behavior of the renormalized amplitudes ($B$ parameters), the conversion of the $B$ parameters from the RI-MOM to the $\overline{\mathrm{MS}}$ scheme and the extrapolation of the results in the heavy-quark mass. These points are all essential to obtain the final results and to estimate the systematic errors. The explicit expressions for the evolution matrices and the corrections relating different schemes have been derived from the results of [20, 21].

### 3.1 Scale dependence of the $B$ parameters

The renormalized operators obtained non-perturbatively are subject to systematic errors. It is thus important to check whether the renormalized matrix elements follow the scaling behavior predicted by NLO perturbation theory. This is also important because we finally have to compute the physical amplitudes by combining our matrix elements with the Wilson coefficients evaluated using perturbation theory in [4].

The scaling behavior of the matrix elements is governed by the following equation (we use the same notation as in [20])

$$\langle \mathbf{Q}(\mu_2)\rangle = W^T[\mu_2,\mu_1]^{-1}\langle \mathbf{Q}(\mu_1)\rangle, \tag{26}$$

where the evolution operator $W[\mu_2,\mu_1]$ can be written as

$$W[\mu_2,\mu_1] = M(\mu_2)U(\mu_2,\mu_1)M^{-1}(\mu_1). \tag{27}$$

$U(\mu_2,\mu_1)$ is the leading order matrix and the NLO corrections are encoded in $M(\mu)$. For our purpose, it is convenient to rewrite (27) in the following form

$$W[\mu_2,\mu_1] = w(\mu_2)w^{-1}(\mu_1), \tag{28}$$

where

$$w(\mu) = M(\mu)\alpha_{\mathrm{s}}(\mu)^{-\gamma_0^T/2\beta_0}, \tag{29}$$

and $\beta_0 = 11 - 2n_f/3$. The one-loop anomalous dimension is scheme independent and, in the basis (22), it is given by

$$\gamma_0 = \begin{pmatrix} -28/3 & 4/3 \\ 16/3 & 32/3 \end{pmatrix}.$$

The NLO contribution

$$M(\mu) = \widehat{1} + J^{n_f}_{\mathrm{RI-MOM}}\frac{\alpha_{\mathrm{s}}(\mu)}{4\pi} \tag{30}$$

is given in terms of the matrix $J^{n_f}_{\mathrm{RI-MOM}}$, which we write explicitly for $n_f = 0$

$$J^{n_f=0}_{\mathrm{RI-MOM}} = \begin{pmatrix} \frac{170749}{27225} + \frac{44}{9}\log 2 & -\frac{247372}{27225} + \frac{28}{9}\log 2 \\ -\frac{6667}{27225} + \frac{28}{9}\log 2 & -\frac{196424}{27225} + \frac{44}{9}\log 2 \end{pmatrix}, \tag{31}$$

since our lattice results are obtained in the quenched approximation. These formulae are sufficient for the study of the scaling behavior of $B'_S(\mu)$ and $\tilde{B}'_S(\mu)$. For $B_S(\mu)$ and $\tilde{B}_S(\mu)$, since they are obtained by dividing the operator matrix elements by $\langle \hat{P}_5(\mu)\rangle = \langle 0|\hat{P}_5(\mu)|P\rangle$, we also need the NLO evolution of the pseudoscalar density with the scale $\mu$, in the RI-MOM scheme and with $n_f = 0$. This is given by

$$\langle \hat{P}_5^{\mathrm{RI-MOM}}(\mu_2)\rangle = \left(\frac{\alpha_{\mathrm{s}}(\mu_2)}{\alpha_{\mathrm{s}}(\mu_1)}\right)^{-4/11} \times \left(1 - \frac{489}{242}\frac{\alpha_{\mathrm{s}}(\mu_2) - \alpha_{\mathrm{s}}(\mu_1)}{\pi}\right)\langle \hat{P}_5^{\mathrm{RI-MOM}}(\mu_1)\rangle. \tag{32}$$

We now use the above formulae to check whether our lattice results scale as predicted by perturbation theory.

**Table 3.** Results for $B'_S(\mu)$ and $\tilde{B}'_S(\mu)$ in the Landau RI-MOM scheme. The light-quark mass is extrapolated/interpolated to $d/s$ quarks

| $\mu$ | 1.9 GeV | | 2.7 GeV | | 3.8 GeV | |
|---|---|---|---|---|---|---|
| Light quark | $q=s$ | $q=d$ | $q=s$ | $q=d$ | $q=s$ | $q=d$ |
| $B'_S(\mu;\kappa_Q=0.1250)$ | 0.93(3) | 0.98(5) | 1.15(4) | 1.21(6) | 1.32(4) | 1.38(7) |
| $\tilde{B}'_S(\mu;\kappa_Q=0.1250)$ | 0.99(4) | 1.06(6) | 1.21(4) | 1.29(6) | 1.41(5) | 1.49(7) |
| $B'_S(\mu;\kappa_Q=0.1220)$ | 0.83(3) | 0.85(4) | 1.02(3) | 1.05(5) | 1.17(4) | 1.20(5) |
| $\tilde{B}'_S(\mu;\kappa_Q=0.1220)$ | 0.87(3) | 0.91(5) | 1.06(3) | 1.10(5) | 1.23(4) | 1.28(6) |
| $B'_S(\mu;\kappa_Q=0.1190)$ | 0.75(2) | 0.77(3) | 0.91(2) | 0.94(4) | 1.05(3) | 1.08(4) |
| $\tilde{B}'_S(\mu;\kappa_Q=0.1190)$ | 0.77(3) | 0.82(4) | 0.94(3) | 0.99(4) | 1.10(3) | 1.15(5) |

**Table 4.** As in Table 3, but for $B_S(\mu)$ and $\tilde{B}_S(\mu)$

| $\mu$ | 1.9 GeV | | 2.7 GeV | | 3.8 GeV | |
|---|---|---|---|---|---|---|
| Light quark | $q=s$ | $q=d$ | $q=s$ | $q=d$ | $q=s$ | $q=d$ |
| $B_S(\mu;\kappa_Q=0.1250)$ | 0.87(3) | 0.84(4) | 0.85(2) | 0.82(3) | 0.87(2) | 0.79(3) |
| $\tilde{B}_S(\mu;\kappa_Q=0.1250)$ | 0.92(3) | 0.91(4) | 0.90(3) | 0.88(4) | 0.88(3) | 0.86(4) |
| $B_S(\mu;\kappa_Q=0.1220)$ | 0.90(3) | 0.85(4) | 0.88(2) | 0.83(3) | 0.85(2) | 0.80(3) |
| $\tilde{B}_S(\mu;\kappa_Q=0.1220)$ | 0.94(3) | 0.91(4) | 0.92(2) | 0.88(4) | 0.90(2) | 0.86(4) |
| $B_S(\mu;\kappa_Q=0.1190)$ | 0.92(2) | 0.91(3) | 0.90(2) | 0.89(3) | 0.87(2) | 0.86(3) |
| $\tilde{B}_S(\mu;\kappa_Q=0.1190)$ | 0.95(3) | 0.96(4) | 0.93(2) | 0.94(3) | 0.91(2) | 0.91(3) |

In Fig. 4, we plot the evolution of both $B'_S(\mu)$ and $B_S(\mu)$, by normalizing them at one of the scales at which we have computed the renormalization matrix $Z_{ij}$ in (22).

From the figure, we see that $B'_S(1.9\,\text{GeV})$ falls below the other results. On the other hand, the evolution curves relative to $B'_S(\mu = 2.7\,\text{GeV})$ and $B'_S(\mu = 3.8\,\text{GeV})$ are closer to each other. This is to be contrasted to the situation for $B_S(\mu)$ where the scale dependence is not as large as for $B'_S(\mu)$, and the description of our data by the perturbative NLO anomalous dimension is more satisfactory, as also shown in Fig. 4. To convert our result to the $\overline{\text{MS}}$ scheme, as central values we choose the $B$ parameters obtained with the non-perturbative renormalization at $\mu = 3.8\,\text{GeV}$. The difference with the other results will be accounted in the systematic uncertainty.

### 3.2 $B$ parameters in the $\overline{\text{MS}}$ scheme at $\mu = m_b$

In [4], the formulae in (2) and (4) were derived in the $\overline{\text{MS}}$ scheme. For this reason we have to convert our results from RI-MOM to $\overline{\text{MS}}$. We have chosen to change the renormalization scheme before extrapolating in the heavy-quark mass. The change of scheme is obtained by using the relation

$$\langle \mathbf{Q}^{\overline{\text{MS}}}(\mu)\rangle = \left(\widehat{1} + r_{\overline{\text{MS}}}\frac{\alpha_s(\mu)}{4\pi}\right)\langle \mathbf{Q}^{\text{RI-MOM}}(\mu)\rangle,$$

where

$$r_{\overline{\text{MS}}} = \frac{1}{18}\begin{pmatrix} 56+88\log 2 & -8+56\log 2 \\ -143+56\log 2 & -115+88\log 2 \end{pmatrix}. \quad (33)$$

We note that $r_{\overline{\text{MS}}}$ is independent of $n_f$. $\langle \mathbf{Q}^{\overline{\text{MS}}}(\mu = 3.8\,\text{GeV})\rangle$ is then evolved to $\mu = m_b = 4.6\,\text{GeV}$ using (26), with $J^{n_f=0}_{\text{RI-MOM}}$ replaced by

$$J^{n_f=0}_{\overline{\text{MS}}} = \begin{pmatrix} \frac{9561}{3025} & -\frac{20723}{18150} \\ \frac{1811}{9075} & -\frac{4997}{6050} \end{pmatrix}. \quad (34)$$

The $\overline{\text{MS}}$ $B$ parameters at $\mu = m_b^{\text{pole}} = 4.6\,\text{GeV}$ are presented in Table 5. $m_b^{\text{pole}} = 4.6\,\text{GeV}$ corresponds to the $\overline{\text{MS}}$ mass given in Table 1 and it is very close to the value used in [4] to evaluate the Wilson coefficients at NLO.

### 3.3 Extrapolation to the $B_s$ meson

From Tables 3, 4 and 5, we observe that the dependence of $B'_S$ on both the renormalization scale and the heavy-quark (meson) mass is much more pronounced than in the case of the parameter $B_S$ (see also Figs. 4 and 5). In particular, because of the large mass dependence, it is more difficult to extrapolate $B'_S$ to the physical point. This is related to the fact that in (18) the ratio $(m_{B_s}/m_b)^2$, distinguishing $B_S$ from $B'_S$, still varies very rapidly in the mass range (around the charm) covered in our simulation. A similar problem is found if one tries to extract $m_b$ from the heavy-meson spectrum, computed with fully propagating quarks, by extrapolating in the heavy-quark mass. For this reason, so far, $m_b$ has been computed on the lattice only by using the heavy quark effective theory (HQET) [22] or non-relativistic QCD (NRQCD) [23]. Thus, although in principle we would prefer $B'_S$ because

**Table 5.** $B$ parameters in the $\overline{\rm MS}$ scheme at $\mu = 4.6\,{\rm GeV}$

| $\kappa_Q$ | 0.1250 | | 0.1220 | | 0.1190 | |
|---|---|---|---|---|---|---|
| Light quark | $q = s$ | $q = d$ | $q = s$ | $q = d$ | $q = s$ | $q = d$ |
| $m_P$ [GeV] | 1.85(7) | 1.75(8) | 2.11(9) | 2.02(9) | 2.38(10) | 2.26(11) |
| $B'_S(m_P, m_b)$ | 1.52(5) | 1.60(8) | 1.35(4) | 1.39(7) | 1.21(3) | 1.25(5) |
| $\tilde{B}'_S(m_P, m_b)$ | 2.18(8) | 2.31(12) | 1.93(6) | 1.99(10) | 1.72(5) | 1.79(8) |
| $B_S(m_P, m_b)$ | 0.73(2) | 0.71(3) | 0.76(2) | 0.72(3) | 0.78(2) | 0.76(3) |
| $\tilde{B}_S(m_P, m_b)$ | 1.05(3) | 1.03(5) | 1.08(3) | 1.03(5) | 1.10(3) | 1.09(5) |

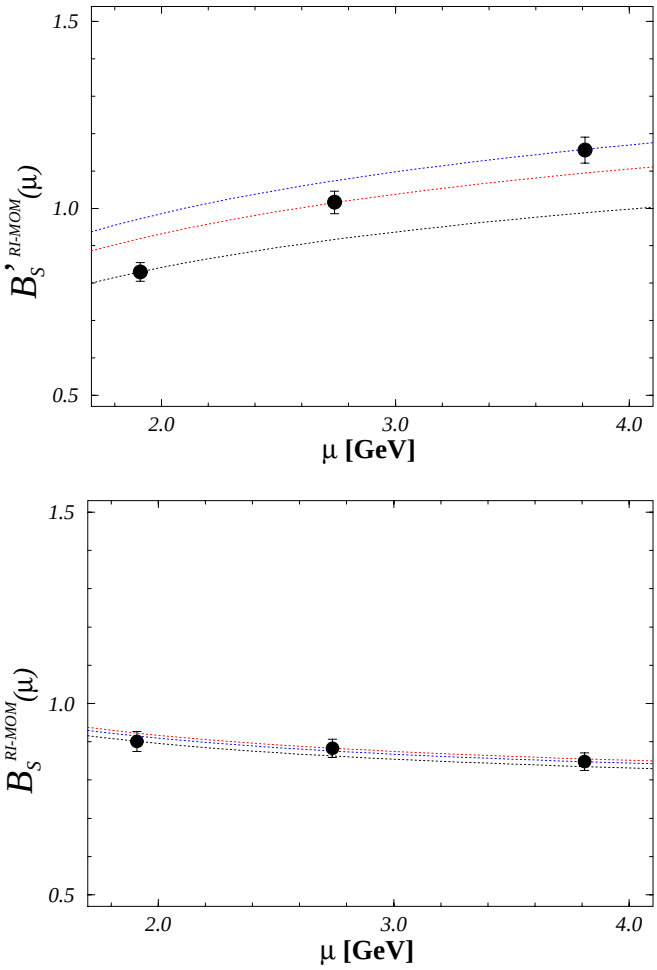


**Fig. 4.** NLO evolution of the parameters $B'_S(\mu)$ and $B_S(\mu)$ in the RI-MOM scheme. The curves are obtained by starting the evolution from the lattice results (filled circles) at $\mu = 1.9$, 2.7 and 3.8 GeV, respectively

it allows the evaluation of the matrix element without using the quark mass, in practice our best results are those obtained from $B_S$. For the same reasons, we were unable to extract $\mathcal{R}(m_b) = \langle Q_S\rangle/\langle Q_L\rangle$ directly from the ratio of the matrix elements. The strongest dependence of $B'_S$ on the quark mass finds its explanation in the framework of the HQET, by studying the leading and subleading contributions in the $1/m_b$ expansion to the $B$ parameters [24]. Our estimates of $(\Delta\Gamma_{B_s}/\Gamma_{B_s})$ are then obtained with $\mathcal{R}(m_b)$ computed by using $B_S$, $B_{B_s}$ and $m_b$ from Table 1, as shown below. For completeness we also present the results for $B'_S$. Hopefully, when smaller values of the lattice spacing, and hence larger values of the heavy-quark mass, will be accessible, an accurate determination of the physical matrix element will be provided by $B'_S$.

In order to make the extrapolation in the heavy-quark mass from the region where we have data to $m_b$, we rely on the scaling laws of the HQET. The $B$ parameters in Table 5 have been obtained using the anomalous dimension matrix of the massless theory. This is the appropriate procedure since, from our data, $\mu$ is larger than the heavy-quark mass, $m_Q$, used in our simulation. In order to use the HQET scaling laws, we have to evolve first to a scale smaller than the quark mass, at $m_Q$ fixed, and then to study the scaling at fixed $\mu$ as a function of the heavy-quark mass. In practice, this is achieved, at LO in the anomalous dimensions, by introducing the following quantities:

$$\mathbf{\Phi}(m_{P_s}, m_b) = \left(\frac{\alpha_{\rm s}(m_{P_s})}{\alpha_{\rm s}(m_{B_s})}\right)^{\gamma/2\beta_0} \mathbf{B}(m_{P_s}, m_b),$$
$$\mathbf{\Phi}'(m_{P_s}, m_b) = \left(\frac{\alpha_{\rm s}(m_{P_s})}{\alpha_{\rm s}(m_{B_s})}\right)^{\gamma'/2\beta_0} \mathbf{B}'(m_{P_s}, m_b), \quad (35)$$

where we have introduced the matrices $\gamma = \gamma_0 - \widetilde{\gamma}_0 + 2(\widetilde{\gamma}_P - \gamma_P)$, and $\gamma' = \gamma_0 - \widetilde{\gamma}_0 + 2\widetilde{\gamma}_A$. $\mathbf{B} = \left(B_S, \tilde{B}_S\right)^T$ and similarly for $\mathbf{B}'$. $\widetilde{\gamma}_0$ is the HQET anomalous dimension matrix which at leading order is given by

$$\widetilde{\gamma}_0 = -\frac{8}{3}\begin{pmatrix} 2 & 1 \\ 1 & 2 \end{pmatrix}, \quad (36)$$

whereas $\widetilde{\gamma}_P = \widetilde{\gamma}_A = -4$ and the LO anomalous dimension of the pseudoscalar density in full QCD is given by $\gamma_P = -8$.

The quantity $\mathbf{\Phi}(m_{P_s}, m_b)$ scales with the heavy-quark (heavy meson) as

$$\mathbf{\Phi}(m_{P_s}, m_b) = \alpha + \frac{\beta}{m_{P_s}} + \ldots \quad (37)$$

The extrapolations of $B_S^{\overline{\rm MS}}(m_b)$ and $B_S'^{\overline{\rm MS}}(m_b)$ to $m_{B_s}$ are shown in Fig. 5. The results are

$$B_S^{\overline{\rm MS}}(m_b) = 0.86(2), \quad \tilde{B}_S^{\overline{\rm MS}}(m_b) = 1.25(3),$$
$$B_S'^{\overline{\rm MS}}(m_b) = 0.63(3), \quad \tilde{B}_S'^{\overline{\rm MS}}(m_b) = 0.91(5). \quad (38)$$

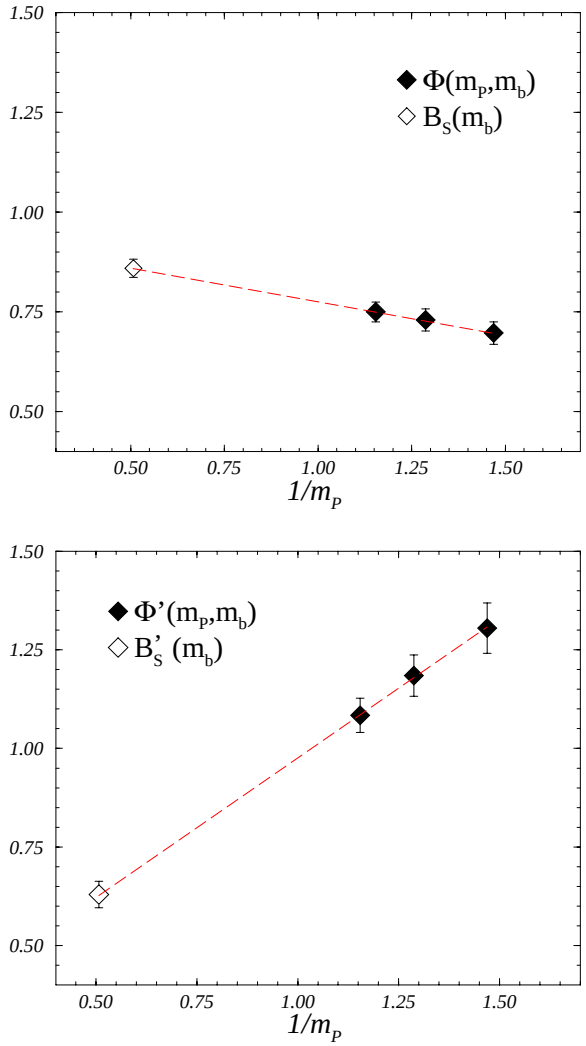


**Fig. 5.** Extrapolation of $\Phi(m_P, m_b)$ and $\Phi'(m_P, m_b)$ in $1/m_P$ to the $B_s$ meson mass. $m_P$ is given in lattice units

As for the systematic uncertainties, we account for the following two.
(1) If, instead of converting to the $\overline{\rm MS}$ scheme before extrapolating to $m_{B_s}$, we extrapolate our RI-MOM results (obtained at $\mu = 3.8\,{\rm GeV}$) in the heavy quark by using the same scaling laws of (35), then evolve to $\mu = m_b$, and convert to the $\overline{\rm MS}$ scheme, the results are[3]

$$B_S^{\overline{\rm MS}}(m_b) = 0.88(2), \quad \tilde{B}_S^{\overline{\rm MS}}(m_b) = 1.27(3),$$
$$B_S'^{\overline{\rm MS}}(m_b) = 0.62(3), \quad \tilde{B}_S'^{\overline{\rm MS}}(m_b) = 0.90(5). \tag{39}$$

(2) If we start from a $\mu$ lower than 3.8 GeV, for example $\mu = 1.9\,{\rm GeV}$, then $B_S(m_b)$ and $\tilde{B}_S(m_b)$ change by $-3\%$, while $B'_S(m_b)$ and $\tilde{B}'_S(m_b)$ drop by $-6\%$.

[3] If the last conversion from the RI-MOM to the $\overline{\rm MS}$ scheme is made by using $n_f = 4$ the results remain remarkably stable (they decrease by about 1%)

After combining these uncertainties, we arrive at our final results:

$$B_S^{\overline{\rm MS}}(m_b) = 0.86(2)^{+0.02}_{-0.03}, \quad \tilde{B}_S^{\overline{\rm MS}}(m_b) = 1.25(3)^{+0.02}_{-0.05},$$
$$B_S'^{\overline{\rm MS}}(m_b) = 0.63(3)^{+0.00}_{-0.04}, \quad \tilde{B}_S'^{\overline{\rm MS}}(m_b) = 0.91(5)^{+0.00}_{-0.06}. \tag{40}$$

From these numbers, we observe that there is a discrepancy between the value of $B_S^{\overline{\rm MS}}(m_b)$ and $B'_S{}^{\overline{\rm MS}}(m_b)$. Using $B_S'^{\overline{\rm MS}}(m_b) \simeq (m_{B_s}/m_b)^2 B_S^{\overline{\rm MS}}(m_b)$, with $(m_{B_s}/m_b)^2 = 1.6$ from Table 1, we get $B'_S{}^{\overline{\rm MS}}(m_b) \sim 1.37$, which is about twice the value of $B_S'^{\overline{\rm MS}}(m_b)$ in (40).

In order to obtain the physical results we have used $B_S^{\overline{\rm MS}}(m_b)$, for which the extrapolation to the $B_s$ meson is much smoother. In this case, we are obliged to use the quark mass to derive the matrix element needed to obtain $\mathcal{R}(m_b)$, which is the relevant quantity for $(\Delta\Gamma_{B_s}/\Gamma_{B_s})$, as explained in the introduction. This is not a major concern, however, since $m_b$ is known with a very tiny error (see Table 1).

The best way to minimize the statistical uncertainty is to compute on the same set of configurations

$$\frac{B_S^{\overline{\rm MS}}(m_b)}{B_{B_s}^{\overline{\rm MS}}(m_b)} = 0.95(3)^{+0.00}_{-0.02}, \tag{41}$$

which, when combined with the numbers from Table 1, gives the wanted quantity

$$\mathcal{R}(m_b) = -\frac{5}{8}\left(\frac{m_{B_s}}{m_b(m_b)+m_s(m_b)}\right)^2 \frac{B_S(m_b)}{B_{B_s}(m_b)}$$
$$= -0.93(3)^{+0.00}_{-0.01}. \tag{42}$$

## 4 Conclusion

In this section, we compare our results with previous lattice studies and find that we can draw the following conclusion.

First lattice calculations of $B_S(\mu)$ were performed in [25,26], using the (unimproved) Wilson fermion action. In [26] the $B$ parameters were obtained in a modified $\overline{\rm MS}$ NDR scheme, at the scale $\mu = 2.33\,{\rm GeV}$, at a heavy-quark mass corresponding approximately to the $D_s$ mass. By translating the result of the authors of [26] to the $\overline{\rm MS}$ of [6], one finds $B_S^{\overline{\rm MS}}(2.33\,{\rm GeV}) = 0.81(1)$ and $\tilde{B}_S^{\overline{\rm MS}}(2.33\,{\rm GeV}) = 0.86(1)$. To compare with these numbers, we have used our results at $\kappa_Q = 0.1250$, interpolated to the strange light-quark mass and then evolved down to $\mu = 2.33\,{\rm GeV}$. We get $B_S^{\overline{\rm MS}}(2.33\,{\rm GeV}) = 0.80(2)$ and $\tilde{B}_S^{\overline{\rm MS}}(2.33\,{\rm GeV}) = 1.05(2)$. $B_S^{\overline{\rm MS}}$ is hence in very good agreement with the value of [26], whereas our $\tilde{B}_S^{\overline{\rm MS}}$ is 20% larger. We note, however, that the values $B_S^{\overline{\rm MS}}(2.33\,{\rm GeV}) = 0.81$ and $\tilde{B}_S^{\overline{\rm MS}}(2.33\,{\rm GeV}) = 0.86$ correspond (only evolution but no extrapolation in the heavy-quark mass) to $B_S^{\overline{\rm MS}}(m_b) = 0.75$ [6] which is 14% smaller than our number.

In [17,27], NRQCD has been used to compute $B'_S(m_b)$. A comparison with them is interesting, because effective theories have different systematic errors with respect to the approach followed in the present study. Their latest result (which we convert to $B_S$) reads $B_S^{\overline{\rm MS}}(m_b) = 0.78(2)(10)$, which is in fair agreement with ours. Moreover their ratio $B_S^{\overline{\rm MS}}(m_b)/B_{B_s}^{\overline{\rm MS}}(m_b) \sim 0.78/0.85 = 0.92$ is very close to ours. This implies that, in spite of the difference in the single $B$ parameters, the same physical answer for $(\Delta\Gamma_{B_s}/\Gamma_{B_s})$ is obtained from (8). In [17,27], in order to get the width difference, these authors adopted, however, another expression ((4) of [27]), which uses different inputs, namely the experimental inclusive semileptonic branching ratio and the theoretical determination of the decay constant $f_{B_s} = 245 \pm 30\,\mathrm{MeV}$. Their result [17], $(\Delta\Gamma_{B_s}/\Gamma_{B_s}) = (10.7 \pm 2.6 \pm 1.4 \pm 1.7) \times 10^{-2}$, is about a factor of two larger than ours. One may wonder whether the difference is due to a different evaluation of the $1/m$ corrections, which are so important in this game. From our calculation, we find that this contribution to $(\Delta\Gamma_{B_s}/\Gamma_{B_s})$ is about $-8.6 \times 10^{-2}$, identical to the value used in [17,27] ((9) of [27]). Besides the fact that these authors use a formula which involves the inclusive semileptonic branching ratio, the main difference stems, instead, from the use of a very large value of $f_{B_s}$ (and to a lesser extent from the use of $m_b = 4.8\,\mathrm{GeV}$ instead of $4.6\,\mathrm{GeV}$). We do not find it justified to use the *unquenched* value of $f_{B_s}$, combined with $B$ parameters computed in the quenched approximation. What really matters is the combination of these quantities in the matrix elements, and we do not know how much the $B$ parameters change in the unquenched case. This is the reason why we prefer (8), which does not require $f_{B_s}$, but only $\mathcal{R}(m_b)$ (which is essentially the same for us and in [17]) and $\xi$, which is known to remain almost the same in the quenched and unquenched case [10].

On the lattice, physical quantities relevant in heavy-quark physics can be computed following two main routes, either by extrapolating the results in the heavy-quark mass from a region around the charm mass or by using some effective theory (HQET or NRQCD). The two approaches have different systematics and in many cases lead to results which are barely compatible. The $B_s$ width difference is particularly lucky, in this respect, since $\mathcal{R}(m_b)$ in our calculation and in [17] are in excellent agreement and lead to the same value of $(\Delta\Gamma_{B_s}/\Gamma_{B_s})$ if (8) is used. It is not surprising that the authors of [17] predict a much larger value for $(\Delta\Gamma_{B_s}/\Gamma_{B_s})$, since they use a very large value of $f_{B_s}$, which is not needed in (8). We find that, in order to reduce the present error, a better determination of the $1/m$ correction, although rather hard to make, is very important. Obviously, calculations with larger heavy-quark masses and without quenching are also demanded for a better control of the remaining systematic errors.

*Acknowledgements.* We warmly thank E. Franco and O. Schneider, for discussions. V. G. has been supported by CICYT under the Grant AEN-96-1718, by DGESIC under the Grant PB97-1261 and by the Generalitat Valenciana under the Grant GV98-01-80. We acknowledge the M.U.R.S.T. and the INFN for support.

## References

1. R. Barate et al. [ALEPH Collaboration], CERN-EP-2000-036
2. O. Schneider, talk given at "35th Rencontres de Moriond", Les Arcs, France, 11–18 March 2000, [hep-ex/0006006]
3. V.A. Khoze, M.A. Shifman, N.G. Uraltsev, M.B. Voloshin, Sov. J. Nucl. Phys. **46**, 112 (1987)
4. M. Beneke, G. Buchalla, I. Dunietz, Phys. Rev. D **54**, 4419 (1996), [hep-ph/9605259]
5. I. Dunietz, Eur. Phys. J. C **7**, 197 (1999), [hep-ph/9806521]
6. M. Beneke, G. Buchalla, C. Greub, A. Lenz and U. Nierste, Phys. Lett. B **459**, 631 (1999), [hep-ph/9808385]
7. A.J. Buras, M. Jamin, P.H. Weisz, Nucl. Phys. B **347**, 491 (1990)
8. T. Inami, C.S. Lim, Prog. Theor. Phys. **65**, 297 (1981)
9. The LEP B Oscillation Working Group, LEPBOSC 98/3
10. S. Hashimoto, review talk given at the 17th International Symposium on Lattice Field Theory "Lattice '99", Pisa, Italy, 29 June–3 July 1999, [hep-lat/9909136]
11. D. Becirevic, D. Meloni, A. Retico, V. Gimenez, L. Giusti, V. Lubicz, G. Martinelli, [hep-lat/0002025]
12. M. Ciuchini, E. Franco, L. Giusti, V. Lubicz, G. Martinelli, Nucl. Phys. B **573**, 201 (2000), [hep-ph/9910236]
13. M. Lüscher, Les Houches Lectures on "Advanced Lattice QCD", and references therein [hep-lat/9802029]
14. G. Martinelli, C. Pittori, C.T. Sachrajda, M. Testa, A. Vladikas, Nucl. Phys. B **445**, 81 (1995), [hep-lat/9411010]
15. A. Donini et al., Phys. Lett. B **360**, 83 (1996 ); M. Crisafulli et al., Phys. Lett. B **369**, 325 (1996); A. Donini et al., Phys. Lett. B **470**, 233 (1999), [hep-lat/9910017]; L. Conti et al., Phys. Lett. B **421**, 273 (1998), [hep-lat/9711053]
16. A. Donini, V. Gimenez, G. Martinelli, M. Talevi, A. Vladikas, Eur. Phys. J. C **10**, 121 (1999), [hep-lat/9902030]
17. S. Hashimoto, K.I. Ishikawa, T. Onogi, M. Sakamoto, N. Tsutsui, N. Yamada, [hep-lat/0004022]
18. D. Becirevic, P. Boucaud, V. Gimenez, V. Lubicz, G. Martinelli, J. Micheli, M. Papinutto, Phys. Lett. B **487**, 74 (2000), [hep-lat/0005013]
19. A. Donini, V. Gimenez, L. Giusti, G. Martinelli, Phys. Lett. B **470**, 233 (1999), [hep-lat/9910017]
20. M. Ciuchini, E. Franco, V. Lubicz, G. Martinelli, I. Scimemi, L. Silvestrini, Nucl. Phys. B **523**, 501 (1998), [hep-ph/9711402]
21. A.J. Buras, M. Misiak, J. Urban, [hep-ph/0005183]
22. V. Gimenez, G. Martinelli, C.T. Sachrajda, Phys. Lett. B **393**, 124 (1997), [hep-lat/9607018]; G. Martinelli, C.T. Sachrajda, Nucl. Phys. B **559**, 429 (1999), [hep-lat/9812001]; V. Gimenez, L. Giusti, G. Martinelli, F. Rapuano, JHEP **0003**, 018 (2000), [hep-lat/0002007]
23. C.T. Davies et al., Phys. Rev. Lett. **73**, 2654 (1994), [hep-lat/9404012]; A. Ali Khan et al., [hep-lat/9912034]
24. V. Gimenez, J. Reyes, in preparation
25. M. Lusignoli, G. Martinelli, A. Morelli, Phys. Lett. B **231**, 147 (1989)
26. R. Gupta, T. Bhattacharya, S. Sharpe, Phys. Rev. D **55**, 4036 (1997), [hep-lat/9611023]
27. S. Hashimoto, K.I. Ishikawa, T. Onogi, N. Yamada, [hep-ph/9912318]